THE JOURNAL OF BIOLOGICAL CHEMISTRY VOL. 281, NO. 33, pp. 23620–23631, August 18, 2006
Printed in the U.S.A.

Arsenic Induces NAD(P)H-quinone Oxidoreductase I by Disrupting the Nrf2·Keap1·Cul3 Complex and Recruiting Nrf2·Maf to the Antioxidant Response Element Enhancer*

Received for publication, May 1, 2006, and in revised form, June 7, 2006 Published, JBC Papers in Press, June 19, 2006, DOI 10.1074/jbc.M604120200

Xiaoqing He, Michael G. Chen, Gary X. Lin, and Qiang Ma[1]

From the Receptor Biology Laboratory, Toxicology and Molecular Biology Branch, Health Effects Laboratory Division, National Institute for Occupational Safety and Health, Centers for Disease Control and Prevention, Morgantown, West Virginia 26505

The ubiquitous toxic metalloid arsenic elicits pleiotropic adverse and adaptive responses in mammalian species. The biological targets of arsenic are largely unknown at present. We analyzed the signaling pathway for induction of detoxification gene NAD(P)H-quinone oxidoreductase (*Nqo1*) by arsenic. Genetic and biochemical evidence revealed that induction required cap 'n' collar basic leucine zipper transcription factor Nrf2 and the antioxidant response element (ARE) of *Nqo1*. Arsenic stabilized Nrf2 protein, extending the $t_{1/2}$ of Nrf2 from 21 to 200 min by inhibiting the Keap1·Cul3-dependent ubiquitination and proteasomal turnover of Nrf2. Arsenic markedly inhibited the ubiquitination of Nrf2 but did not disrupt the Nrf2·Keap1·Cul3 association in the cytoplasm. In the nucleus, arsenic, but not phenolic antioxidant *tert*-butylhydroquinone, dissociated Nrf2 from Keap1 and Cul3 followed by dimerization of Nrf2 with a Maf protein (Maf G/Maf K). Chromatin immunoprecipitation demonstrated that Nrf2 and Maf associated with the endogenous *Nqo1* ARE enhancer constitutively. Arsenic substantially increased the ARE occupancy by Nrf2 and Maf. In addition, Keap1 was shown to be ubiquitinated in the cytoplasm and deubiquitinated in the nucleus in the presence of arsenic without changing the protein level, implicating nuclear-cytoplasmic recycling of Keap1. Our data reveal that arsenic activates the Nrf2/Keap1 signaling pathway through a distinct mechanism from that by antioxidants and suggest an "on-switch" model of *Nqo1* transcription in which the binding of Nrf2·Maf to ARE controls both the basal and inducible expression of *Nqo1*.

Environmental toxic metal arsenic, which originates from both geochemical and anthropogenic activities, is a ubiquitous contaminant and an established human carcinogen (1, 2). Arsenic has become a major public health concern worldwide because millions of people are at risk of drinking water contaminated with arsenic that has been associated with multiple human diseases or lesions (3–5). The anthropogenic sources of arsenic contaminating soil and water include mining, metallurgical activities, and manufacture and agricultural use of pesticides and herbicides. Arsenic causes a spectrum of adverse responses in many species. Whereas acute exposure to inorganic arsenic in humans results in cardiac failure, peripheral neuropathy, anemia, leucopenia, and death, chronic arsenic exposure can cause a range of cancers (particularly of the skin, lung, bladder, and liver) as well as liver injury, neuropathy, cardiovascular lesions, ovarian dysfunction, aberrant embryo development, and postnatal growth retardation (4, 6–10). Interestingly, arsenic-containing compounds have proven to be effective as therapeutic agents in treating cancer such as leukemia (11), chronic inflammatory disease such as psoriasis (12), and parasitic infection such as sleeping sickness (13, 14). Although chemical interaction with protein thiol groups and generation of reactive oxygen species have been implicated in the actions of arsenic, the exact molecular targets and signaling pathways that account for most of the biological effects of arsenic remain unknown.

The ubiquity in the environment and the pleiotropy of toxicity of arsenic have provided selective pressure for evolution of various strategies across species that are utilized to defend against the toxic metal. For instance, high level resistance to arsenite in *Escherichia coli* is conferred by the *arsRDABC* operon of plasmid R773, which controls the efflux of the metal through a tightly regulated, arsenic sensing/transcription repression mechanism (15). In mammals, arsenic can be methylated by arsenic methyltransferase (16). Methylated arsenics have a shorter half-life *in vivo* than inorganic arsenic. However, As(III)-containing methylated metabolites have been shown to be more cyto- and genotoxic than either arsenate or arsenite (17). Given the high potency and wide range of biological effects of arsenic, it is perceivable that complex regulatory mechanisms other than methylation exist to control cellular homeostasis in mammalian cells exposed to the soft metal.

Certain detoxification enzymes metabolize chemicals through reduction and conjugation reactions to less toxic and more water-soluble metabolites. In addition, the enzymes such as NQO1[2] directly or indirectly participate in the metabolism of

* The costs of publication of this article were defrayed in part by the payment of page charges. This article must therefore be hereby marked "*advertisement*" in accordance with 18 U.S.C. Section 1734 solely to indicate this fact.

[1] To whom correspondence should be addressed: Receptor Biology Laboratory, TMBB/HELD/NIOSH/CDC, Mailstop 3014, 1095 Willowdale Rd., Morgantown, WV 26505. Tel.: 304-285-6241; Fax: 304-285-5708; E-mail: qam1@cdc.gov.

[2] The abbreviations used are: NQO1, NAD(P)H-quinone oxidoreductase; Nrf2, nuclear factor erythroid 2-related factor 2; ARE, antioxidant response element; tBHQ, *tert*-butylhydroquinone; CHX, cycloheximide; IP, immunoprecipitation; ChIP, chromatin immunoprecipitation; DAPI, 4′,6-diamidino-2-phenylindole; Cul3, Cullin 3; E3, ubiquitin-protein isopeptide ligase; PBS, phosphate-buffered saline; HA, hemagglutinin; Pipes, 1,4-piperazinediethanesulfonic acid; Ub, ubiquitin.

reactive oxygen species (18). Many of the genes, exemplified by *Nqo1*, are induced by a wide range of oxidative and electrophilic chemicals through the antioxidant response element (ARE) located in the enhancers of the genes (19, 20). This ARE paradigm of gene regulation is shared by a second set of enzymes/proteins, including heme oxygenase 1, glutathione synthetase, and γ-glutamylcysteine synthetase that combat against reactive oxygen species and other stress signals (21).

The cap 'n' collar basic leucine zipper protein Nrf2 (nuclear factor erythroid 2-related factor 2) is a member of the leucine zipper family of transcription factors. Genetic and biochemical studies have uncovered an essential function of Nrf2 in the regulation of ARE-controlled gene transcription (19, 22, 23). Nrf2 is required for both the basal and inducible expression of a number of ARE-controlled genes. Dormant Nrf2 resides in the cytoplasm and is rapidly turned over through the ubiquitin-26 S proteasome pathway. The cytoplasmic Nrf2-binding protein Keap1 controls the ubiquitination of Nrf2 through the Cullin 3 (Cul3)-dependent ubiquitin ligase (E3) (24–26). Moreover, Keap1 interacts with oxidative or electrophilic chemicals through its thiol groups in the linker region between the BTB (BR-C, ttk and bab) and Kelch domains for activation of Nrf2 by inducers (27). Activated Nrf2 translocates into the nucleus, binds to ARE of target genes, and commences transcription of the genes. Together with the ARE-regulated target genes, the Nrf2·Keap1 regulatory system constitutes a complex and tightly regulated chemical sensing/transcriptional gene regulation mechanism critical in defense against both endogenous and environmental toxic insults. Consistent with this notion, loss of Nrf2 function is associated with increased sensitivity to a number of toxicants, carcinogens, and certain disease processes (21, 28–30). Conversely, activation of Nrf2 has been implicated in chemoprotection against cancer, chemical toxicity, and chronic diseases by natural and synthetic chemoprotective agents (31). The role and mechanism of action of the Nrf2·Keap1·ARE gene system in the transcriptional response to toxic metals has not been well understood.

In an attempt to identify the molecular targets and pathways of protective responses to arsenic, we found that arsenic potently induced detoxification gene *Nqo1* through the Nrf2/ARE-dependent gene transcription. Induction involved a sequential and dynamic protein-protein and protein-DNA interactions. Arsenic stabilized the Nrf2 protein by inhibiting the E1-dependent ubiquitination and subsequent proteasomal turnover of Nrf2, extending the $t_{1/2}$ of Nrf2 from 21 to 200 min. Nrf2 was associated with Keap1 and Cul3 in the cytoplasm. Although both the cytoplasmic Nrf2 and Keap1 were ubiquitinated, arsenic potently inhibited the ubiquitination of Nrf2 but not of Keap1. In the nucleus, treatment with arsenic but not phenolic antioxidant *tert*-butylhydroquinone (tBHQ) dissociated Nrf2 from Keap1·Cul3. Keap1 was ubiquitinated in the cytoplasm and deubiquitinated in the nucleus. Arsenic induced the dimerization of nuclear Nrf2 and Maf (Maf G/Maf K). Chromatin immunoprecipitation (ChIP) analysis revealed that both Nrf2 and Maf are present at the ARE enhancer of *Nqo1* at a low level to mediate the basal transcription. Arsenic treatment substantially increased the occupancy of both Nrf2 and Maf at ARE to control the induction of the gene. On the contrary, AP-1 proteins c-Jun and c-Fos or Nrf2-binding proteins Keap1 and Cul3 were not associated with ARE. The findings revealed differential mechanisms of Nrf2 action by arsenic and antioxidants and provided a mechanistic framework of induction of ARE-driven genes by toxic metals through the Nrf2·Keap1 pathway.

EXPERIMENTAL PROCEDURES

Cell Culture and Treatment—Mouse hepa1c1c7 cells were provided by Dr. J. P. Whitlock, Jr. (Stanford University, Stanford, CA). The cells were grown in α-minimal essential medium with 10% fetal bovine serum and 5% CO_2. Mouse *Nrf2*$^{+/+}$ and *Nrf2*$^{-/-}$ embryonic fibroblast cells were derived from wild type and *Nrf2* null mice as described previously (19). The cells were cultured in Dulbecco's modified Eagle's medium with 10% fetal bovine serum and 5% CO_2. The E36 and ts20 cells (kindly provided by Dr. R. R. Kopito, Stanford University) were grown in Dulbecco's modified Eagle's medium supplemented with 10% fetal bovine serum at 31 °C as described (32). Penicillin (100 units/ml) and streptomycin (100 μg/ml) were added to the media to prevent contamination. Cells at confluency were treated with reagents as specified in figure legends. Sodium arsenite ($NaAsO_2$), dimethyl sulfoxide (Me_2SO), tBHQ, and cycloheximide (CHX) were purchased from Sigma-Aldrich. Me_2SO was used as the solvent control. MG132 was from BioMol (Plymouth, PA).

RNA Preparation and Northern Blotting—Total RNA was isolated from cells using the Qiagen total RNA isolation kit (Qiagen, Valencia, CA). Total RNA of 3 μg each was fractionated in a 1.2% agarose-formaldehyde gel, transferred to a supercharged nylon membrane, and blotted with a digoxigenin (DIG)-labeled riboprobe prepared with the DIG-labeling reagents (Roche Applied Science). Template cDNAs for generating riboprobes of mouse *Nqo1*, *Nrf2*, and actin were verified by sequencing. Northern signals were visualized by chemiluminescence using a digoxigenin RNA detection kit with CDP Star as a substrate (Roche Applied Science). Actin was probed to control loading variations among samples. Results shown were repeated in two to three separate experiments with consistent observations.

Plasmid Construction and Transfection—The full-length coding cDNA of mouse *Nrf2* and *Keap1* were obtained by reverse transcription and PCR from total RNA of hepa1c1c7 cells and was verified by sequencing. *Nrf2* cDNA was subcloned into pCMV-HA (BD Clontech, Palo Alto, CA) at the SfiI and SalI sites to generate pCMV-HA-Nrf2. Keap1 cDNA was subcloned into pcDNA3.1/V5-His (Invitrogen) at the XhoI and ApaI sites to give rise to pKeap1/pcDNA3-V5. The *Nqo1* ARE reporter construct was kindly provided by Drs. K. Itoh and M. Yamamoto (University of Tsukuba, Tsukuba, Japan). The chimeric reporter contains the ARE enhancer from −865 to −897 base pairs upstream of the transcription start of the mouse *Nqo1* gene fused to a β-globin promoter and luciferase cDNA. The reporter plasmid and pCMV-HA-Nrf2 were transfected into hepa1c1c7 cells using the Lipofectamine Plus reagents from Invitrogen per the manufacturer's instructions. To detect ubiquitination of plasmid-expressed Nrf2, pCMV-HA-Nrf2, and pCW-ubiquitin-Myc (kindly provided by Dr. P. Zhou,

Weill Medical College of Cornell University, New York) were co-transfected into cells. Ubiquitination of Nrf2 was examined by immunoblotting as described in the legends to Figs. 5 and 6. Keap1-V5 was expressed in hepa1c1c7 cells by transfection of pKeap1/pcDNA3-V5.

Cell Fractionation, Immunoprecipitation, and Immunoblotting—Nuclear and cytoplasmic fractions were prepared using the Nuclei EZ PREP reagents from Sigma. Briefly, cells at 90% confluency in 10-cm dishes were washed with ice-cold phosphate buffered saline (PBS) and lysed with ice-cold Nuclei EZ PREP lysis buffer containing protease and phosphatase inhibitors (1 mM phenylmethylsulfonyl fluoride, 1 mM Na_3VO_4, 1 mM NaF, and 1 μg/ml concentrations each of aprotinin, leupeptin, and pepstatin A, all added immediately before use). For detection of ubiquitinated proteins, *N*-ethylmaleimide (Pierce) was added to the cell lysis buffer to inhibit ubiquitin-conjugating enzyme. The cell lysate was centrifuged at 500 $\times$ *g* for 5 min at 4 °C to give rise to nuclei (pellet fraction) and cytosol (supernatant fraction). The nuclei pellets were washed once with the lysis buffer and resuspended in a radioimmune precipitation assay buffer (50 mM Tris-HCl, pH 7.4, with 1% Nonidet P-40, 0.25% sodium deoxycholate, 1 mM EDTA; protease and phosphatase inhibitors were added as described above). The nuclear and cytoplasmic fractions were stored at −80 °C till use.

For immunoblotting, cells were washed twice with ice-cold PBS and lysed on ice with the radioimmune precipitation assay buffer with protease and phosphatase inhibitors for 30 min. The cell lysate was sonicated briefly and centrifuged at 14,000 $\times$ *g* for 20 min to remove cell debris. Cell lysate (10 μg), nuclear (5–10 μg), or cytoplasmic (30 μg) proteins were fractionated on 10% SDS-PAGE, transferred to polyvinylidene difluoride membranes (Bio-Rad), and blocked with 5% nonfat milk in PBS plus 0.05% Tween 20. The membranes were blotted with primary antibodies at 4 °C overnight with shaking followed by incubation with horseradish peroxidase-conjugated second antibodies for 1 h at room temperature. Protein bands were visualized using enhanced chemiluminescence detection reagents from Amersham Biosciences. Actin was blotted to ensure equal loading.

For immunoprecipitation (IP), cell lysates or cell fractions were precleared with protein G-agarose (Invitrogen) for 1 h at 4 °C followed by incubation with IP antibodies at 4 °C overnight with shaking. Immune complexes were precipitated by incubation with protein G-agarose at 4 °C for 1 h and a brief centrifugation. The precipitates were washed extensively with PBS plus 0.05% Tween 20 and subjected to fractionation by SDS-PAGE. Protein bands were detected by immunoblotting with specific antibodies as specified in figure legends. Data shown were representatives from two to three separate experiments.

Antibodies against Nrf2, Keap1, Cul3, c-Myc, heme oxygenase 1, Maf G/Maf K, c-Jun, or c-Fos were purchased from Santa Cruz Biotechnology, Inc. (Santa Cruz, CA). The antibodies were routinely tested for specificity, titers, and applications by comparing immunoblotting of the endogenous proteins, *in vitro* transcription-translation-produced products, and transient expression of tagged proteins, respectively; the antibodies recognize corresponding proteins as a single protein band with the same apparent molecular weight by immunoblotting (Figs. 2, 4, 8, and 9 and data not shown). The antibody against HA tag was obtained from Berkeley Antibody Co., Richmond, CA). Anti-ubiquitin antibody, from Zymed Laboratories Inc. (South San Francisco, CA), recognizes conjugated and unconjugated ubiquitins. Anti-V5 was from Invitrogen. Anti-lamin A and anti-glyceraldehyde-3-phosphate dehydrogenase were from Santa Cruz Biotechnology; the anti-lamin A rabbit polyclonal antibody is specific for lamin A and does not cross-react with lamin C.

Cycloheximide Chase Experiment—Regulation of the steady state level and the half-life ($t_{1/2}$) of Nrf2 was analyzed by immunoblotting and CHX chase. Cells were grown to 90% confluence in 35-mm dishes and treated with MG132 (15 μM) for 2 h followed by washing with PBS 3 times. For steady state Nrf2 levels, the cells were treated with arsenic (10 μM) or water (solvent control). Cell lysates were prepared at 0, 0.5, 1, 2, 4, 6, 12, and 24 h after treatment. For CHX chase, the cells were treated with CHX (40 μg/ml) with or without arsenic (10 μM). Cell lysates were prepared at 0, 5, 10, 20, 30, 60, 120, and 240 min after treatment. 10 μg of total protein was fractionated on SDS-PAGE and blotted with antibody against Nrf2. Actin was blotted to ensure equal loading.

Immunofluorescence and Confocal Microscopy—Hepa1c1c7 cells were seeded in a Lab-Tek 4-well chamber slide (Nalge Nunc International Corp. Napervill, IL) in α-minimal essential medium with 10% fetal bovine serum and cultured overnight to 70% confluence. The cells were treated with Me_2SO, tBHQ (30 μM), or arsenic (10 μM) for 5 h. The cells were gently washed with PBS and fixed with ice-cold 4% paraformaldehyde PBS solution for 10 min and permeabilized with 0.2% Triton X-100 PBS solution for 15 min. After washing 3 times with ice-cold PBS, the cells were incubated with anti-Keap1 goat polyclonal antibody (Santa Cruz Biotechnology) for 1 h followed by incubation with Alexa 594-conjugated donkey anti-goat IgG (Red, Molecular Probes, Eugene, Oregon) for another hour. After washing three times with cold PBS, the slide was mounted with mounting solution with DAPI (4′,6-diamidino-2-phenylindole; Vector Laboratories, Burigame, CA) counterstaining to visualize the nuclei (blue). The cells were observed with a confocal microscope (LSM 510, Carl Zeiss, Thornwood, NY) with the multitrack rhodamine-DAPI setting.

ChIP Assay—Hepa1c1c7 cells were treated with arsenic or tBHQ for 5 h. ChIP assay was performed as described previously (33) with modifications. Briefly, DNA-proteins were cross-linked by incubating cells with 1% formaldehyde at 37 °C for 10 min. Excess formaldehyde was quenched with 0.125 M glycine at room temperature. Cells were collected in 1 ml of a lysis buffer (5 mM Pipes, pH 8.0, 85 mM KCl, and 0.5% IGEPAL CA-630) with protease inhibitors and centrifuged to pellet nuclei. The nuclei were resuspended in the lysis buffer, repelleted, and resuspended in a nuclei lysis buffer (50 mM Tris/HCl, pH 8.0, 10 mM EDTA, and 1% SDS) with protease inhibitors. Chromatin was sonicated to an average size of 200–1000 bp using a tapered microtip at 40% power output. Cell debris was removed by centrifugation at a top speed at 4 °C. Sheared chromatin was diluted in an IP dilution buffer (0.01% SDS, 1.1% Triton X-100, 1.2 mM EDTA, 16.7 mM Tris/HCl, pH 8.0, and 167 mM NaCl) precleared with protein G containing salmon sperm DNA (240 μg of sperm DNA in 1 ml of solution) and immunoprecipitated with antibodies as described

under "Experimental Procedures." DNA-protein complexes were eluted from the protein G-agarose beads with an elution buffer 200 μl (50 mM $NaHCO_2$ and 1% SDS) and reverse cross-linked by incubating with 8 μl of 5 M NaCl at 65 °C overnight. The DNA samples were purified and analyzed by real-time PCR using SYBR GREEN PCR master mix (Applied Biosystems, Foster City, CA) performed on a Bio-Rad iCycler (Bio-Rad) following standard procedures. Briefly, for each reaction, DNA template, forward and reverse primers (10 μM each), SYBR Green PCR Master Mix, and water were added to make a final volume of 50 μl. Thermal cycling was carried out as follows: 95 °C for 3 min as initial denaturing followed by 45 cycles of 94 °C for 30 s, 60 °C for 30 s, and 72 °C for 60 s and a final extension at 72 °C for 2 min. Threshold cycles (C_T values) were determined using the iCycler IQ software (Bio-Rad). Real-time PCR results were normalized using 1% of input as an internal control. Relative DNA amounts were calculated from C_T values for each sample by interpolating into the standard curve obtained using a series dilution of standard DNA samples run under the same conditions.

Primer sets used for real-time PCR were as follows: *Nqo1* ARE forward, 5′ GCAGTTTCTAAGAGCAGAACG and reverse, 5′ GTAGATTAGTCCTCACTCAGCCG; *Nqo1* coding region forward, 5′ AACGGGAAGATGTGGAGATG, and reverse, 5′ CGCAGTAGATGCCAGTCAAA. The ChIP assay was routinely performed with two types of negative controls; 1) normal IgG from the same species as each immunoprecipitation antibody and 2) primers specific for the coding region of *Nqo1*.

NQO1 Enzyme Activity Assay—NQO1 activity was performed as described previously (34). Briefly, Hepa1C1C7 cells were seeded in 96-well plates at a density of 2×10^4 cells/ml and cultured overnight. The culture was replaced with fresh medium with different treatments as described in the legend to Fig. 1*B*. After an additional 48 h of culture, the medium was decanted, and the cells were incubated with 50 μl of 0.8% digitonin and 2 mM EDTA solution for 10 min at 37 °C. A reaction mixture was prepared as the following: 0.375 ml of 1 M Tris-HCl, pH 7.4, 10 mg of bovine serum albumin, 0.1 ml of 1.5% Tween 20, 10 μl of 7.5 mM FAD^+ (Sigma), 0.1 ml of 150 mM glucose 6-phosphate (Sigma), 9 μl of 50 mM $NADP^+$ (sigma), 30 units of yeast glucose-6-phosphate dehydrogenase (Sigma), 4.4 mg of 3-(4,5-dimethylthiazol-2-yl)-2,5-diphenyltetrazolium bromide (Sigma), 15 μl of 50 mM menadione (Sigma, added just before use), and distilled water to a volume of 15 ml. 200 μl of the reaction mixture were added to each well for 5 min, and the reaction was stopped by adding a stop solution containing 0.3 mM dicoumarol in 0.5% Me_2SO and 5 mM potassium phosphate, pH 7.4. Absorbance at 595 nm was measured using a 96-well plate reader.

Data Quantification and Statistical Analysis—Quantification of RNA or protein bands were performed using the ImageQuant program (GE Healthcare). The half-life of Nrf2 was calculated with the one-phase exponential decay formula using the GraphPad PRISM program (GraphPad Software, Inc., San Diego, CA). Statistical analysis was performed with one way analysis of variance followed by *t* test using the GraphPad PRISM program.

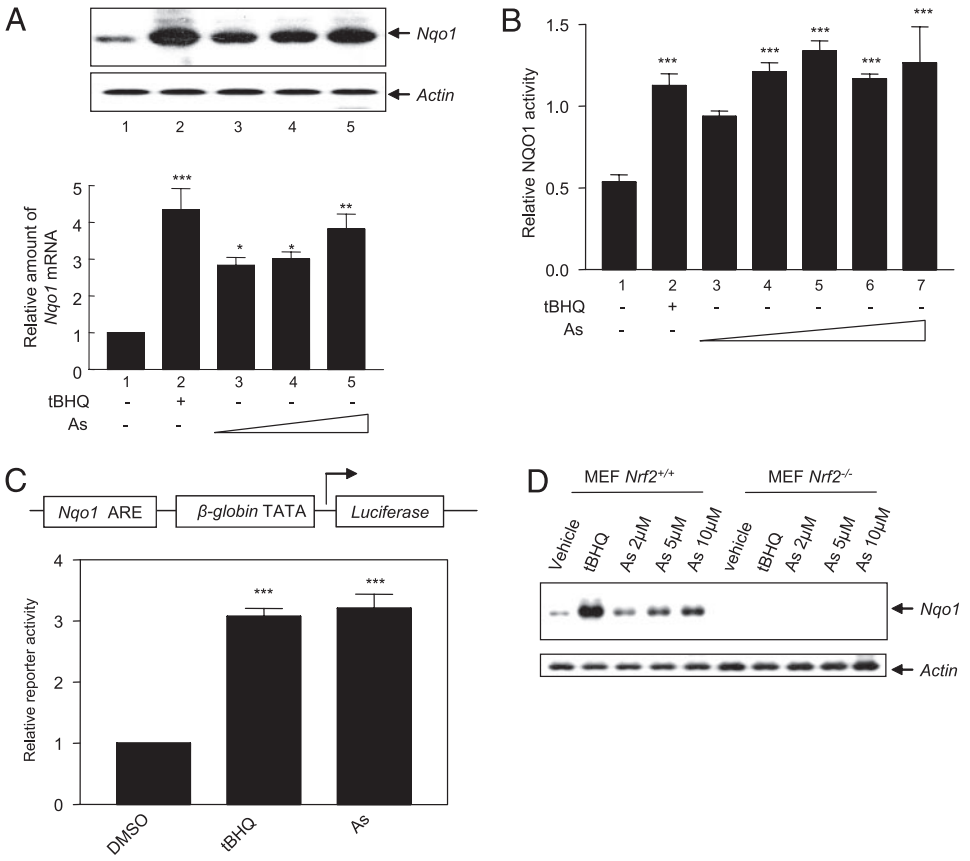

FIGURE 1. **Induction of *Nqo1* through the Nrf2/ARE pathway by arsenic.** *A*, induction of *Nqo1* mRNA. Hepa1c1c7 cells were treated with Me_2SO (vehicle), tBHQ (30 μM), or arsenic (*As*) at 2, 5, and 10 μM for 5 h. Total RNA of 3 μg each was analyzed by Northern for *Nqo1* mRNA expression; actin mRNA was measured to ensure equal loading. *Upper panels*, Northern blotting. *Lower panel*, quantification of Northern blots. *B*, induction of NQO1 enzyme activity. Cells were treated with Me_2SO, tBHQ (30 μM), or arsenic at 0.1, 1, 2, 5, and 10 μM for 48 h. Total cell lysate was prepared, and NQO1 activity was measured. *C*, induction of ARE-luciferase by arsenic. Cells were transfected with plasmids pCMV-HA-Nrf2, pNqo1 ARE/Luc, and the Renilla construct (Promega, as an internal control for transfection) followed by induction with tBHQ (30 μM) or arsenic (10 μM) for 5 h. Cell lysate was prepared, and luciferase activity was measured using the dual luciferase assay protocol. *DMSO*, Me_2SO. *D*, *Nrf2* dependence of *Nqo1* induction. Mouse embryonic fibroblast cells (*MEF*) of wild type (*Nrf2*$^{+/+}$) or knock-out (*Nrf2*$^{-/-}$) were treated with tBHQ (30 μM) or arsenic at 2, 5, and 10 μM for 5 h. Northern blotting of *Nqo1* and actin mRNA was performed. Quantitative data represent the means ± S.D. from three experiments. *, $p < 0.05$; **, $p < 0.01$; ***, $p < 0.001$.

RESULTS

Arsenic Potently Activates the Nrf2/ARE Pathway by Stabilizing Nrf2—Examining induction of a panel of cellular defense genes by arsenic revealed that arsenic robustly induced the

mRNA expression of xenobiotic-metabolizing enzyme NQO1 in hepa1c1c7, a mouse hepatoma cell line with minimal deviation from hepatocytes and highly responsive to arsenic (Fig. 1*A*). Detectable expression of *Nqo1* was apparent in the absence of an inducer (*lane 1*). tBHQ, a prototype of antioxidant inducers, was used as a positive control. tBHQ induced *Nqo1* by 4.5-fold (*lane 2*; 30 μM, 5 h). Arsenic at 2 μM (5 h) induced the gene by 3-fold (*lane 3*). A dose-dependent increase in *Nqo1* induction was observed between 2 and 10 μM arsenic with a maximal induction at 10 μM. Higher concentrations of arsenic were not included to avoid potential toxicity to the cells. Induction of *Nqo1* mRNA was accompanied by elevation of NQO1 enzyme activities (Fig. 1*B*). Because arsenic induced high levels of expression of both mRNA and enzyme activity of *Nqo1* at 2 μM, arsenic is ~15 times as potent as tBHQ in the induction, suggesting induction of *Nqo1* as a suitable model for analyzing the molecular mechanism of transcriptional regulation of ARE-driven genes by arsenic.

To analyze the pathway of *Nqo1* induction by arsenic, we examined the role of ARE. A chimeric reporter construct expressing luciferase under the control of *Nqo1* ARE and a minimal β-globin promoter was transfected into hepa1c1c7 cells. Expression of luciferase was induced by arsenic at 10 μM to the same magnitude as that by tBHQ at 30 μM (~3-fold; Fig. 1*C*), indicating that *Nqo1* ARE is sufficient to support induction of transcription by arsenic in a manner analogous to the induction of endogenous *Nqo1*.

Induction of ARE-driven reporter implicates Nrf2 in *Nqo1* induction by arsenic. A genetic approach was utilized to test the notion. Embryonic fibroblasts were derived from *Nrf2* null (mouse embryonic fibroblast cells (MEF) $Nrf2^{-/-}$) and wild type mice (MEF $Nrf2^{+/+}$). *Nqo1* mRNA was expressed constitutively, and arsenic induced *Nqo1* expression dose-dependently in $Nrf2^{+/+}$ cells (Fig. 1*D*). However, both the basal expression and induction of *Nqo1* by arsenic were lost in $Nrf2^{-/-}$ cells. Expression of actin was not affected by *Nrf2* knock-out. Taken together, arsenic potently induced *Nqo1* through the Nrf2-mediated, ARE-dependent signaling pathway.

Nrf2 has been shown to be regulated at both transcriptional and posttranscriptional levels by antioxidants; thus, we examined the effect of arsenic on *Nrf2* mRNA and protein expression. Arsenic treatment did not affect the expression of *Nrf2* mRNA (Fig. 2*A*). Nrf2 protein was barely detectable in uninduced cells (Fig. 2, *B* and *C*, *lane 1*). Arsenic increased the protein level of Nrf2 in both dose- and time-dependent manners (Fig. 2, *B* and *C*, *lanes 2*–6), indicating a post-transcriptional mechanism of Nrf2 regulation by arsenic. tBHQ at 30 μM increased the Nrf2 protein level similarly to arsenic (Fig. 2*B*; *lane 5*); however, cotreatment with arsenic and tBHQ did not further increase the protein level (compare *lanes 5* and *6*), suggesting a common pathway in Nrf2 regulation by arsenic and tBHQ. The effect of arsenic on the steady state level of the Nrf2 protein was further examined in protein decay experiments. Nrf2 protein was first induced by MG132 (15 μM, 2 h) followed by extensive washing with fresh media to remove the inducer. Immunoblotting of Nrf2 revealed that the protein level of Nrf2 decreased time-dependently in the absence of an inducer with a half-reduction time of ~1.47 h (Fig. 3, *A* and *B*). Treatment with

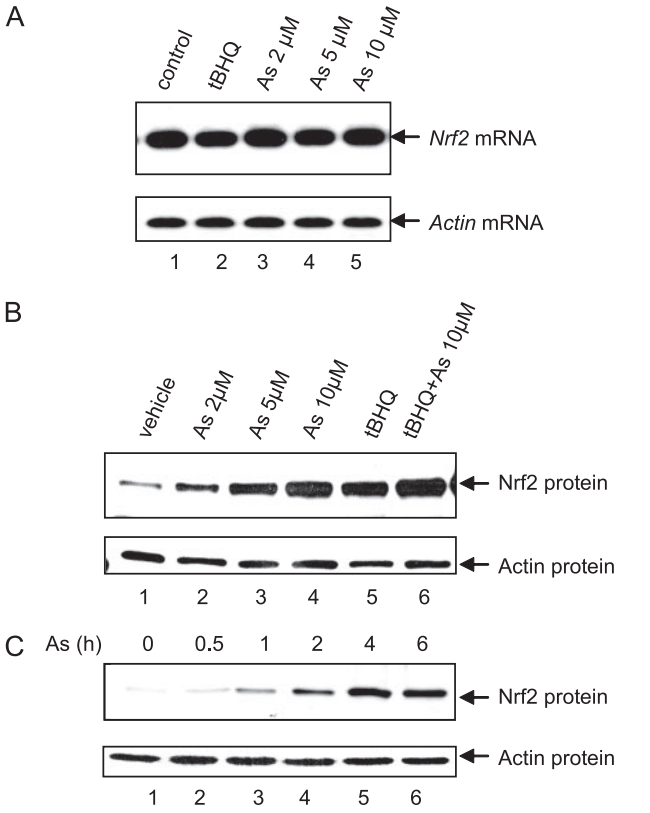

FIGURE 2. **Arsenic (*As*) increases the protein level of Nrf2.** Hepa1c1c7 cells were treated as indicated for 5 h (30 μM tBHQ). *A*, Northern blotting of Nrf2 mRNA. *B*, immunoblotting of Nrf2 protein. *C*, immunoblotting; time curve of arsenic treatment (10 μM).

arsenic extended the half reduction time 4 times longer (~6.02 h). Cycloheximide chase was performed to measure the half-life of the Nrf2 protein. Nrf2 was induced, and then protein synthesis was blocked by treatment with cycloheximide (40 μg/ml). Nrf2 was measured by immunoblotting (Fig. 3, *C* and *D*). In the absence of arsenic, the half-life ($t_{1/2}$) of Nrf2 was 21.08 min; treatment with arsenic increased the $t_{1/2}$ by 10-fold ($t_{1/2}$ = 200 min). The results demonstrated that arsenic increased the protein level of Nrf2 by inhibiting the turnover of Nrf2 protein.

Keap1 anchors Nrf2 in the cytoplasm and regulates Nrf2 degradation. Keap1 was shown to be down-regulated by antioxidants through a non-proteasomal pathway recently (35), whereas in a separate study Keap1 was found to be induced by arsenic in a human keratinocyte cell line (36). We, therefore, examined the regulation of Keap1 by arsenic in hepa1c1c7 cells. The results revealed that treatment with arsenic, tBHQ, or MG132 did not change the expression level of endogenous (Fig. 4*A*) and transfection-expressed (Fig. 4*B*) Keap1 proteins. The anti-Keap1 antibody recognized the endogenous, *in vitro* expressed, and transfection-expressed Keap1 (with V5 tag) proteins as single bands with the same mobility on immunoblotting (Fig. 4, *A* and *B*). To further test the notion that Keap1 is a stable protein, cells were treated with CHX, tBHQ, MG132, or combinations of the agents. Fig. 4*C* revealed that Keap1 protein level was unaffected by blocking of protein synthesis, treatment with antioxidants, or inhibition of proteasomal protein degradation (lower bands), confirming Keap1 as a stable protein. The same membrane was blotted against Nrf2 as an internal control

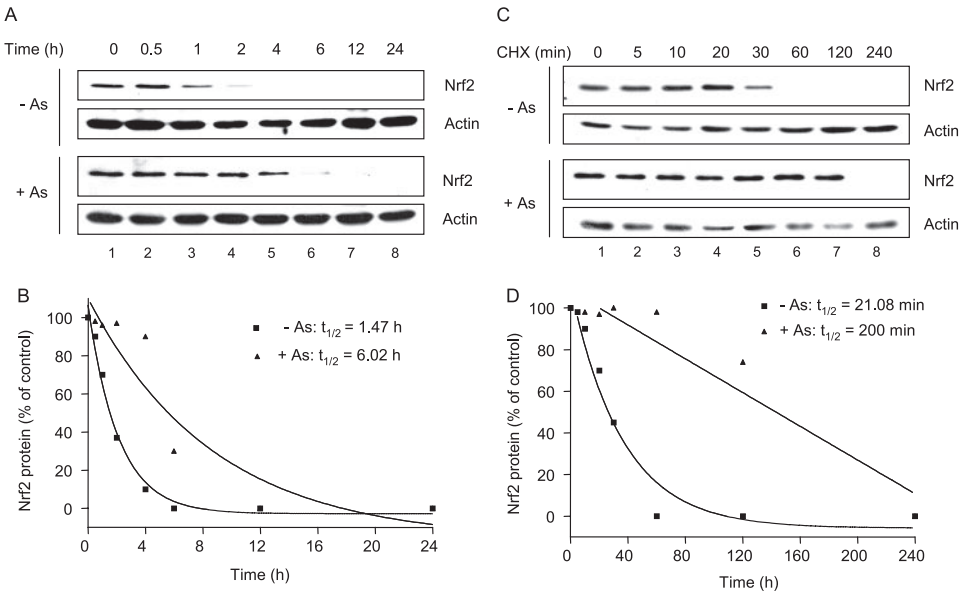

FIGURE 3. **Arsenic inhibits Nrf2 protein turnover.** *A* and *B*, steady state level of Nrf2 protein. Cells were pretreated with MG132 (15 μM, 2 h) followed by extensive washing to remove MG132. The cells were then treated with arsenic (*As*) at 10 μM for the indicated time periods. Nrf2 protein was examined by immunoblotting (*A*) and decay of the Nrf2 protein with or without arsenic was quantitated (*B*). *C* and *D*, CHX chase of Nrf2 protein. Cells were pretreated with MG132 followed by extensive washing. Cells were then treated with CHX (40 μg/ml) with or without arsenic (10 μM) for the indicated time periods. *C*, immunoblotting of Nrf2 and actin. *D*, quantitative plot of Nrf2 protein turnover.

to show that CHX was effective in diminishing the protein level of Nrf2 (*upper bands*). Immunoconfocal microscopy revealed that endogenous Keap1 was present in both the cytoplasm and nucleus; moreover, treatment with tBHQ or arsenic did not affect the fluorescent levels of Keap1 in the two cellular compartments (Fig. 4*D*). This conclusion was further confirmed by immunoblotting of cytoplasmic and nuclear extracts (see Fig. 6). Together, the data indicated that modulation of the protein level of Nrf2 but not Keap1 serves as a major target of arsenic action.

Arsenic Disrupts the Nrf2·Keap1·Cul3 Complex in the Nucleus—To analyze the pathway by which arsenic regulates Nrf2 turnover, ts20 (temperature-sensitive E1 mutant) and E36 (wild type) cells were examined. At 31 °C (permissive to E1 function in ts20), Nrf2 is nearly undetectable in both ts20 and E36 cells (Fig. 5*A*; *lane 1*). Treatment with tBHQ, MG132 (an inhibitor of the 26 S proteasomes), or arsenic increased Nrf2, with the highest level of increase by MG132 (*lanes 2–4*). At 42 °C (impermissible for E1 in ts20), the basal level of Nrf2 was dramatically increased in ts20, but not E36 cells (*lane 5*), indicating that E1 was required for the short $t_{1/2}$ of Nrf2 in the cells. The result is in agreement with previous findings that Nrf2 is rapidly degraded through the ubiquitin-26 S proteasome pathway in the absence of an inducer (19, 24). The Nrf2 levels at the elevated temperature in ts20 cells treated with tBHQ, MG132, or arsenic were all comparable with each other and with that of vehicle treatment, suggesting that a maximal stabilization of Nrf2 was reached in the absence of E1 function. On the contrary, the Nrf2 levels in E36 cells treated with vehicle, tBHQ, MG132, or arsenic were similar to those at 31 °C, consistent with the presence of a functional E1 in the cells at both temperatures. These findings suggest that arsenic inhibits Nrf2 degradation by modulating the E1-dependent, 26 S proteasome pathway of Nrf2 turnover.

To directly detect inhibition of Nrf2 ubiquitination by arsenic, Nrf2 with a HA tag and ubiquitin with a c-Myc tag were expressed in hepa1c1c7 cells. Nrf2 was immunoprecipitated with anti-HA and detected with anti-c-Myc (Fig. 5*B*). High levels of ubiquitinated Nrf2 were detected in vehicle or MG132-treated cells (*lanes 1* and *3*), whereas arsenic and tBHQ reduced the level of ubiquitinated Nrf2 (*lanes 4* and *2*). Reduction of ubiquitinated Nrf2 was not due to reduced levels of Nrf2 (*middle panel*) or variation of protein loading (*lower panel*) since the protein levels of HA-Nrf2 and actin were comparable among the treatments. Ubiquitinated Nrf2 was also immunoprecipitated with anti-Nrf2 or anti-Ub and immunoblotted with anti-Ub or anti-Nrf2, respectively. In either of the scenarios, ubiquitinated Nrf2 was detected in vehicle-, tBHQ-, or arsenic-treated cells in a similar manner to that of Fig. 5*B* (data not shown).

To analyze the interplay among Nrf2, ubiquitination, and the Keap1·Cul3 ligase complex, we examined the ubiquitination of endogenous Nrf2 and Keap1 as well as the association of Nrf2 with the E3 components in the cytoplasmic and nuclear compartments. Hepa1c1c7 cytoplasmic and nuclear fractions were prepared with high purity as shown by the absence of lamin A (a nuclear marker) and presence of glyceraldehyde-3-phosphate dehydrogenase (a cytoplasmic marker) in the cytoplasmic faction (*left*) and the presence of lamin A and absence of glyceraldehyde-3-phosphate dehydrogenase in the nuclear fraction (*right*) (Fig. 6*A*, *bottom two panels*). Treatment with tBHQ or arsenic increased the Nrf2 protein in the cytoplasm (*first panel*, *left*, *lanes 2* and *3*); the protein levels were further increased in the nucleus (*right*, *lanes 2* and *3*), consistent with stabilization and nuclear enrichment of the proteins upon the treatments. Pretreatment with MG132 followed by tBHQ or arsenic substantially increased Nrf2 protein to a similar level among the treatments in both fractions, reflecting the potent stabilizing effect of MG132 on Nrf2 protein (*left* and *right panels*, *lanes 4–6*). In contrast, tBHQ, arsenic, MG132, or the cotreatments did not change the protein levels of Keap1 or Cul3, indicating that they are stable proteins (*second* and *third panels*).

In the cytoplasm, low but detectable levels of ubiquitinated Nrf2 and Keap1 were observed in arsenic- or tBHQ-treated cells (Fig. 6*B*, *upper left panel*). Pretreatment with MG132 dramatically increased the level of ubiquitinated Nrf2 (*lane 4*). However, the level was decreased by treatment with arsenic; the decrease reflects inhibition of ubiquitination of Nrf2 since the

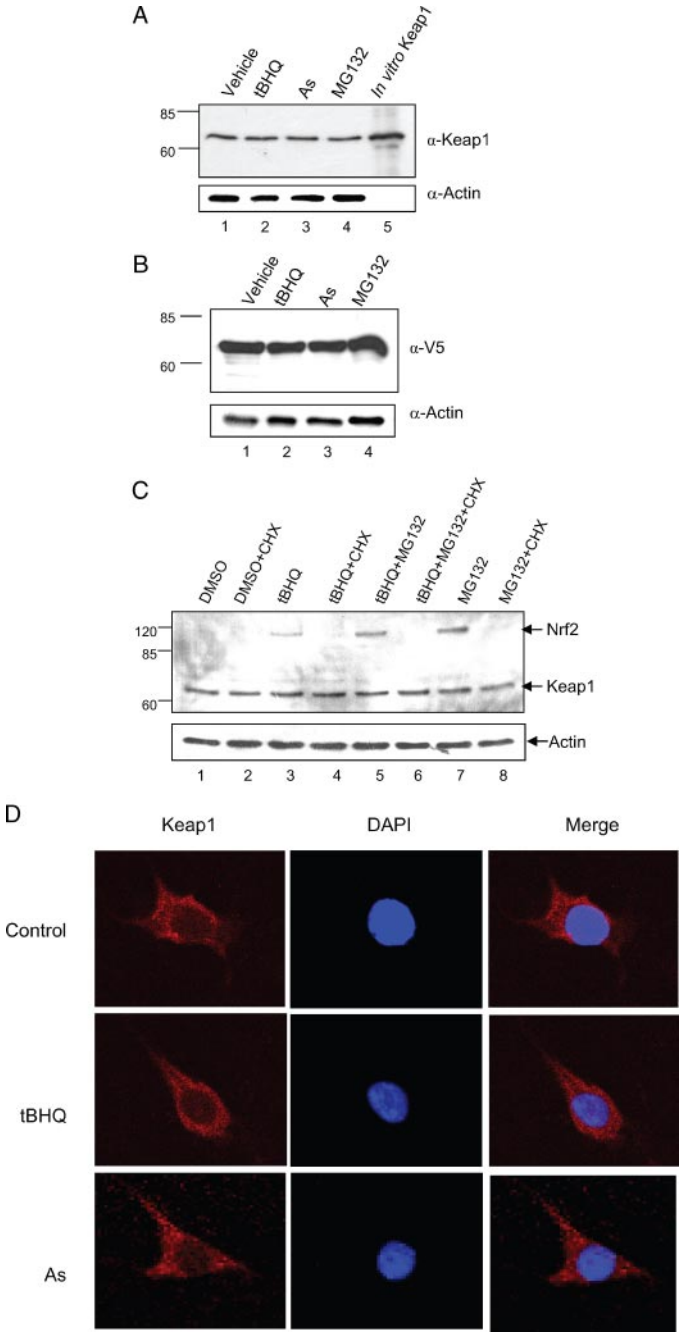

FIGURE 4. **Keap protein stability.** *A*, Hepa1c1c7 cells were treated with tBHQ (30 μM), arsenic (*As*, 10 μM), or MG132 (15 μM) for 5 h. Total cell lysate was immunoblotted with anti-Keap1 antibodies. *Lane 5*, Keap1 produced by *in vitro* transcription and translation. *B*, cells were transfected with pKeap1/pcDNA3-V5. Thirty-six hours later the cells were treated with tBHQ, arsenic, or MG132 as for *A*. Total cell lysate was immunoblotted with anti-V5. *C*, Hepa1c1c7 cells were treated with CHX (10 μg/ml), tBHQ (30 μM), MG132 (15 μM), or in combinations as shown for 5 h. Total cell lysate was sequentially immunoblotted with anti-Keap1 or anti-Nrf2. *DMSO*, Me_2SO. *D*, cellular localization of Keap1. Hepa1c1c7 cells were immunostained with anti-Keap1 and Alexa 594-conjugated second antibodies (*red*) and were counterstained with DAPI to show the nucleus (*blue*). Fluorescence image was taken using confocal microscopy. The *right panels* represent overlay of Keap1 and DAPI fluorescence images.

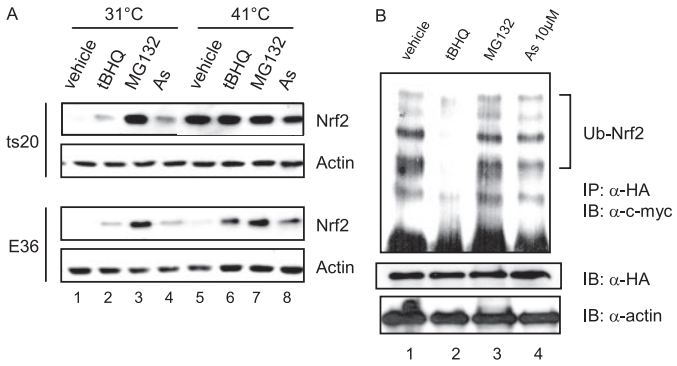

FIGURE 5. **Ubiquitination of Nrf2.** *A*, E1 dependence of Nrf2 turnover. Wild type (E36) and E1 temperature-sensitive mutant (ts20) cells were treated with tBHQ (30 μM), MG132 (15 μM), or arsenic (*As*, 10 μM) at 31 or 41 °C for 4 h. Expression of Nrf2 and actin protein was examined by immunoblotting. *B*, effect of arsenic on Nrf2 ubiquitination. Cells were co-transfected with pCMV-HA-Nrf2 and pCW-ubiquitin-Myc plasmids followed by treatment with tBHQ (30 μM), MG132 (15 μM), or arsenic (10 μM) for 4 h. Total cell lysate was immunoprecipitated with anti-HA and blotted (*IB*) with anti-c-Myc (*upper panel*). The same lysate was immunoblotted with anti-HA or anti-actin for HA-Nrf2 and actin expression levels (*middle* and *lower panels*).

protein levels of Nrf2 were high and were similar to each other among the treatments (Fig. 6*A*, *first panel*, compare *lanes 4–6*). Ubiquitination of Nrf2 was detectable but was substantially lower in the nucleus than in the cytoplasm, even in the presence of MG132 (Fig. 6*B*, *upper right panel*), suggesting deubiquitination of Nrf2 in the nucleus. Interestingly, detectable ubiquitination of Keap1 was found in the cytoplasm similarly to that of Nrf2 (Fig. 6*B*, *lower left panel*). Keap1 ubiquitination was substantially increased by MG132, further supporting Keap1 as an E3 substrate. Unlike Nrf2, however, arsenic or tBHQ did not affect MG132-induced ubiquitination of Keap1. In the nuclear fraction, ubiquitination of Keap1 was dramatically reduced for all treatments than that in the cytoplasmic fraction (*lower left panel*). Fig. 6*D* provides quantification of ubiquitinated Nrf2 (*upper panel*) and Keap1 (*lower panel*) in the cytoplasm and nucleus. Three conclusions can be drawn from these results; (*a*) ubiquitination of Nrf2 and Keap1 mostly occurred in the cytoplasm, (*b*) arsenic strongly inhibited the ubiquitination of Nrf2 but not Keap1 in the cytoplasm, and (*c*) ubiquitination of both Nrf2 and Keap1 was detectable in the nucleus at substantially lower levels than in the cytoplasm, suggesting deubiquitination of the proteins upon nuclear translocation.

Ubiquitination of Nrf2 by the Cul3-based E3 involves association of Nrf2 with Keap1 and Cul3. Interaction between Nrf2 and Keap1 or Cul3 was analyzed by co-immunoprecipitation with anti-Keap1 or anti-Cul3 antibodies from the cytoplasmic and nuclear fractions followed by blotting with anti-Nrf2 (Fig. 6*C*). As expected, Nrf2 was barely detected by co-immunoprecipitation with either of the antibodies in the absence of an inducer (*lane 1*) in both fractions due to the rapid turnover of the protein under basal conditions. Nrf2 was co-immunoprecipitated with Keap1 and Cul3 in the cytoplasm from cells treated with either arsenic or tBHQ (*left panels*; *lanes 3* and *2*), indicating that arsenic or tBHQ stabilized Nrf2 but did not dissociate Nrf2 from the Nrf2·Keap1·Cul3 complex in the cytoplasm. On the other hand, Nrf2 was co-immunoprecipitated with anti-Keap1 or anti-Cul3 from the nuclear fraction of cells treated with tBHQ, but not with arsenic, revealing that treatment with arsenic but not tBHQ resulted in dissociation of Nrf2 from the Nrf2·Keap1·Cul3 complex in the nucleus (*right panels*; compare *lanes 2* and *3*). Keap1 remains associated with Cul3 in

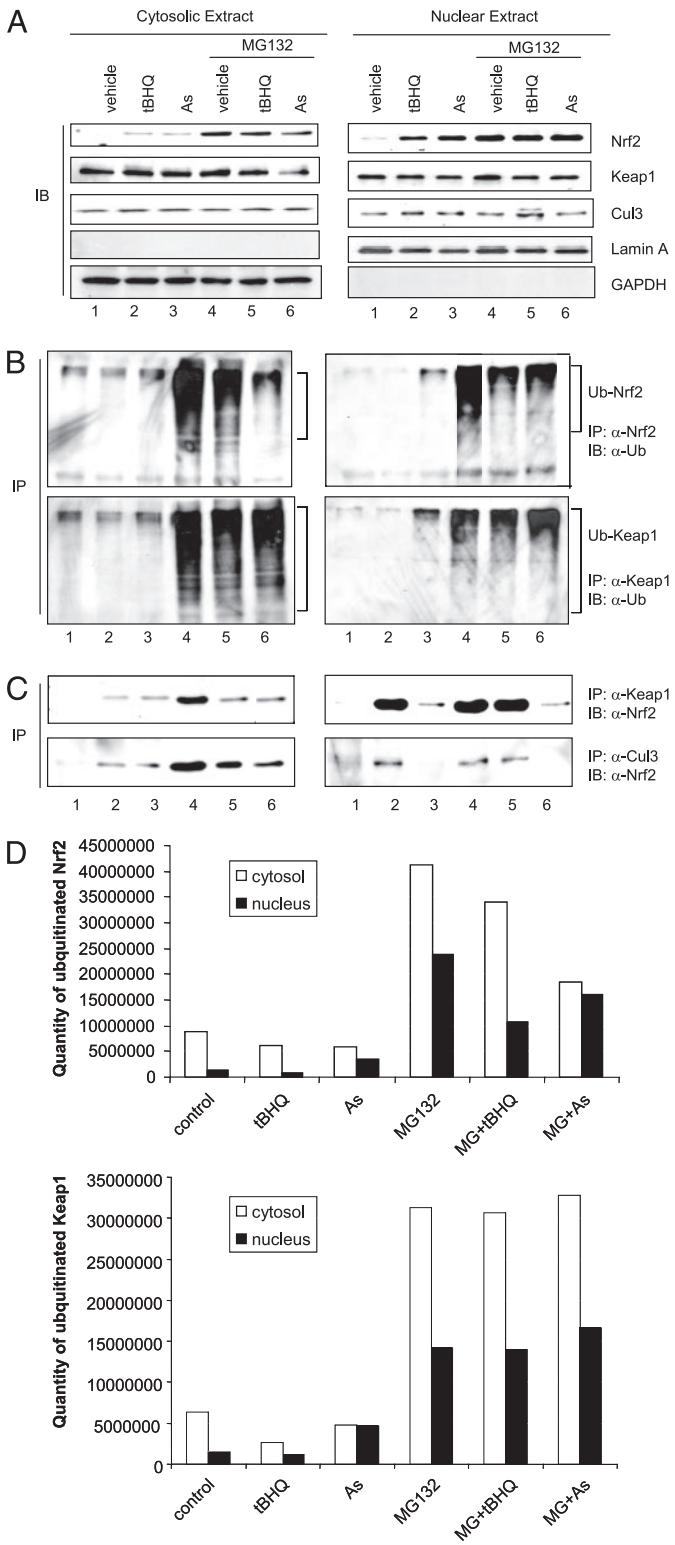

FIGURE 6. **Effect of arsenic on the ubiquitination of endogenous Nrf2 and Keap1 and association of Nrf2 with Keap1 and Cul3 in the cytoplasm and nucleus.** Hepa1c1c7 cells were treated with tBHQ (30 μM), arsenic (*As*, 10 μM), or MG132 (15 μM) for 4 h or pretreated with MG132 for 2 h followed by tBHQ or arsenic for 4 h. Cytoplasmic (*left*) and nuclear (*right*) fractions were prepared. *A*, immunoblotting (*IB*) of cytoplasmic (*left*) and nuclear (*right*) fractions. Purity of fractionation was confirmed by the presence of lamin A and absence of glyceraldehyde-3-phosphate dehydrogenase for the nuclear preparation and vice versa for the cytoplasmic preparation (*lower two panels*). Protein levels of Nrf2, Keap1, and Cul3 of the preparations were examined by immunoblotting. *GAPDH*, glyceraldehyde-3-phosphate dehydrogenase. *B*, ubiquitination of endogenous Nrf2 and Keap1 in the cytoplasm and nucleus. Nrf2 or Keap1 was immunoprecipitated with anti-Nrf2 (*upper panels*) or anti-Keap1 (*lower panels*), respectively, from the cytoplasmic (*left panels*) or nuclear (*right panels*) fractions and were immunoblotted with anti-Ub. *C*, association of Nrf2 with Keap1·Cul3. Association of Nrf2 with Keap1 was examined by co-IP with anti-Keap1 and immunoblotting (*IB*) with anti-Nrf2 (*upper panel*). Association of Nrf2 with Cul3 was assayed by co-IP with anti-Cul3 and immunoblotting with anti-Nrf2 (*lower panel*). *D*, quantification of ubiquitinated Nrf2 or Keap1. Ubiquitinated Nrf2 (*upper panel*) or Keap1 (*lower panel*) was detected by immunoblotting as described in *B*. Quantification was performed using the ImageQuant program.

the nucleus in the presence of arsenic or tBHQ as both proteins can be co-immunoprecipitated with either anti-Keap1 or anti-Cul3 (data not shown).

To further examine the interaction among the proteins, cells were pretreated with MG132 for 2 h followed by arsenic or tBHQ for 4 h; MG132 treatment ensured that the amounts of Nrf2 in the cells were high enough for detection and were at similar levels among the treatments for better comparison (Fig. 6*A*, *first panel*, *lanes 4–6*). In the cytoplasm, treatment with MG132 resulted in an increased association of Nrf2 with Keap1 and Cul3 (Fig. 6*C*, *left panel*, *lane 4*). Arsenic or tBHQ in the presence of MG132 increased the association to a level higher than without MG132 (compare *lanes 6* and *5* with *3* and *2*) but lower than with MG132 alone (compare with *lane 4*). In the nucleus, strong association of Nrf2 with Keap1 and Cul3 was observed in cells treated with MG132 or MG132 plus tBHQ, whereas treatment with arsenic in the presence of MG132 disrupted the association. The findings demonstrated that arsenic (but not tBHQ) not only prevented the formation of the Nrf2·Keap1·Cul3 complex but also disrupted the existing complex induced by MG132 pretreatment in the nucleus, revealing a substantial difference in the activation of Nrf2 by arsenic and tBHQ in the nucleus.

Arsenic Recruits Nrf2 and Maf but Not Keap1, Cul3, Ubiquitin, c-Jun, or c-Fos to the ARE of Nqo1—Nrf2 binds to *Nqo1* ARE in *in vitro* assays (37). However, the protein complex binding to *Nqo1* ARE in the absence and presence of an inducer in intact cells remains controversial. Chromatin immunoprecipitation was performed to probe the interaction of Nrf2 with endogenous *Nqo1* ARE *in vivo*. Hepa1c1c7 cells were treated with vehicle, arsenic, or tBHQ; chromatin DNA sequences bound to Nrf2 were co-immunoprecipitated with anti-Nrf2 and were amplified with primers specific to the ARE region of mouse *Nqo1* by real-time PCR. As shown in Fig. 7, *Nqo1* ARE was co-immunoprecipitated with Nrf2 in the absence of an *Nqo1* inducer; the result is in agreement with the notion that Nrf2 is required for the basal expression of *Nqo1* (Fig. 7*A*, *lane 2*). Treatment with arsenic or tBHQ increased the amount of ARE co-immunoprecipitated with Nrf2 (*lanes 4* and *6*), indicating that arsenic or tBHQ increased the binding of Nrf2 to ARE. Quantification by real-time PCR revealed that arsenic induced a 6-fold increase in binding of Nrf2 to ARE, and tBHQ induced a 9-fold increase over the basal binding (Fig. 7*C*). The ChIP assay was specific for anti-Nrf2, because ARE was not detected in co-immunoprecipitation with normal rabbit IgG, followed by PCR amplification with the ARE primers (Fig. 7, *A*, *lanes 1*, *3*, and *5*, and *B*, *lanes 13–15*). The Nrf2-ARE interaction detected by ChIP is also specific for ARE, because co-immunoprecipita-

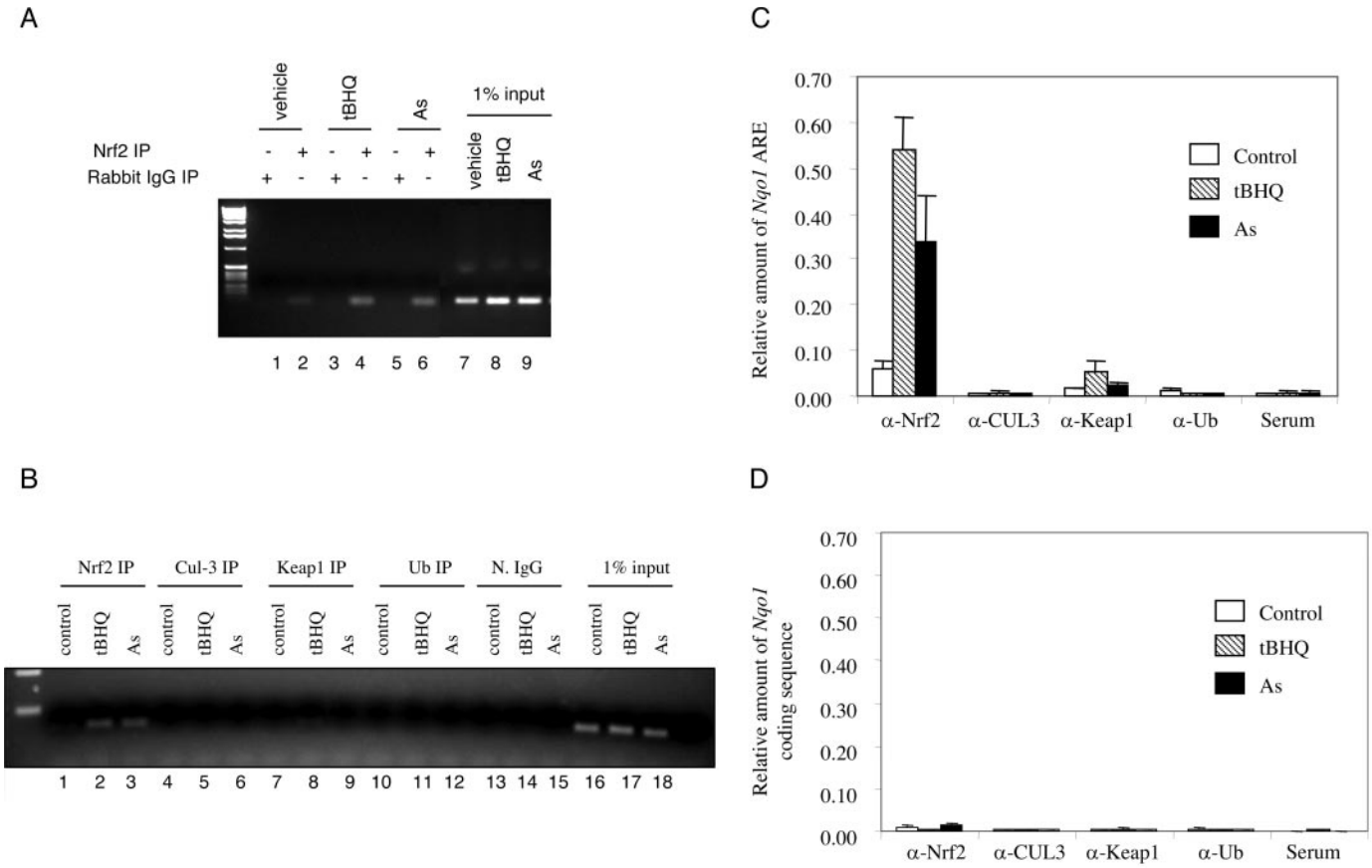

FIGURE 7. **Association of Nrf2, Keap1, Cul3, and ubiquitin with *Nqo1* ARE.** Cells were treated with Me_2SO, tBHQ (30 μM), or arsenic (*As*, 10 μM) for 4 h. *Nqo1* ARE cross-linked to proteins was co-immunoprecipitated with the corresponding antibodies and amplified by real-time PCR with primers specific for mouse *Nqo1* ARE enhancer as described under "Experimental Procedures" (ChIP assay). *A*, ChIP assay of ARE associated with Nrf2. ARE was co-immunoprecipitated with anti-Nrf2 or normal rabbit IgG. 1% of input was shown to normalize input variations for real-time PCR. *B*, ARE association with Cul3, Keap1, and Ub. Association of *Nqo1* ARE with Cul3, Keap1, or Ub was examined by ChIP. Nrf2 and normal IgG (*N. IgG*) were shown as positive and negative controls. 1% of input was shown for equal input of the samples. *C*, quantitative data of ChIP for Nrf2, Cul3, Keap1, and Ub by real-time PCR. *D*, specificity of ARE-protein binding by ChIP assay. Binding of Nrf2, Cul3, Keap1, or Ub to *Nqo1* coding sequence was examined by ChIP with antibodies as indicated. Normal serum was used as a negative control. Bound DNA was amplified by real-time PCR.

tion with anti-Nrf2 followed by PCR amplification with a pair of primers specific for the coding sequence of NQO1 did not detect DNA binding of Nrf2 (Fig. 7*D*).

Because arsenic and tBHQ differentially affect the interaction of Nrf2 with Keap1 and Cul3 in the nucleus, we attempted to determine if Keap1, Cul3, or ubiquitin interacts with endogenous ARE. As shown in Fig. 7, *B* and *C*, ARE was not detected from co-immunoprecipitates with anti-Cul3, anti-Keap1, or anti-Ub (*lanes 4–12*). Anti-Nrf2 and a control serum (*N. IgG*) were used as positive and negative controls for co-immunoprecipitation, respectively. The control serum and antibodies against Cul3, Keap1, or ubiquitin failed to co-immunoprecipitate the *Nqo1* coding sequence as expected (Fig. 7*D*). The results indicated that Nrf2 but not Keap1, Cul3, or ubiquitin was recruited to ARE in the presence of arsenic or tBHQ.

Small Maf proteins, in particular Maf G and Maf K, were shown to heterodimerize with Nrf2 to bind ARE *in vitro* and were suggested to form homodimers in cells to suppress the basal expression of *Nqo1* or heterodimers with Nrf2 to mediate *Nqo1* induction. The role of Maf G/Maf K in the induction of endogenous *Nqo1* by arsenic was examined. Maf G/Maf K was detected only in the nucleus (Fig. 8*A*). Furthermore, the protein levels of Maf G/Maf K were not affected by treatment with tBHQ, arsenic, MG132, or combinations of the agents. Association of Maf K/Maf G with Nrf2 was examined by co-immunoprecipitation (Fig. 8*B*). Arsenic or tBHQ induced the association of Nrf2 with Maf G/Maf K (compare *lanes 3* and *2* with *1*). MG132 strongly increased the association (*lane 4*). Co-treatment with MG132 and arsenic slightly increased the association compared with that by MG132 alone (compare *lanes 6* and *4*). The association in co-treatment with MG132 and tBHQ was substantially lower than that by MG132 or MG132 plus arsenic but was similar to that by tBHQ alone (*lane 5*), consistent with the much smaller effect of tBHQ on nuclear Nrf2·Keap1·Cul3 association than that of arsenic (Fig. 6*C*, *right panel*, compare *lanes 5* and *6*). Finally, the interaction of Maf G/Maf K with the endogenous ARE was examined by ChIP assay with antibodies against Maf G/Maf K. Maf G/Maf K binds to ARE similarly to Nrf2 in the absence of an inducer (Fig. 8*C*). Treatment with arsenic or tBHQ dramatically increased the binding (~5.2 and 8.2-fold, respectively), comparable with the level of binding by Nrf2. Thus, both Nrf2 and Maf G/Maf K bind to ARE constitutively, and both are recruited to *Nqo1* enhancer to increase ARE occupancy upon stimulation by arsenic or tBHQ.

Nqo1 ARE shows a high sequence similarity to the AP-1 binding sequence. Indeed, association of AP-1 proteins with ARE has been suggested previously (38). Possible contributions

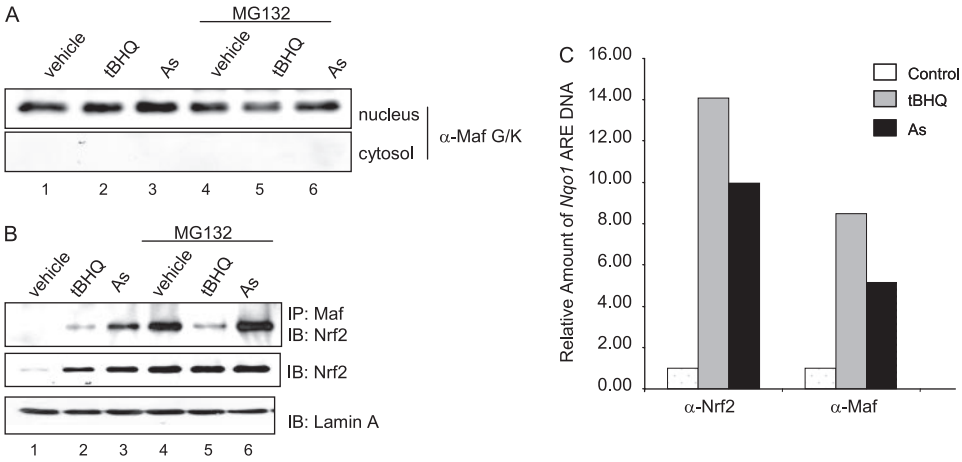

FIGURE 8. **Heterodimerization and association of Nrf2 and Maf K/Maf G with *Nqo1* ARE for basal and inducible expression of *Nqo1*.** *A*, protein expression of Maf G/K. Hepa1c1c7 cells were treated with tBHQ (30 μM), arsenic (*As*, 10 μM), MG132 (15 μM), or MG132 plus tBHQ or arsenic for 4 h. Protein levels of Maf G/Maf K in the cytoplasm and nucleus were examined by immunoblotting. *B*, association of Maf G/Maf K with Nrf2. Cells were treated as described for *A*. Nrf2 and Maf G/Maf K in the nucleus was co-immunoprecipitation with anti-Maf G/Maf K and blotted (*IB*) with anti-Nrf2 (*first panel*). Protein levels of Nrf2 and lamin A (nuclear marker) were examined by immunoblotting (*second* and *third panel*, respectively). *C*, association of Nrf2 and Maf with *Nqo1* ARE. ChIP assay was performed to analyze the association of Maf K/Maf G with *Nqo1* ARE in comparison with Nrf2. Cells were treated with tBHQ (30 μM) or arsenic (10 μM) for 4 h.

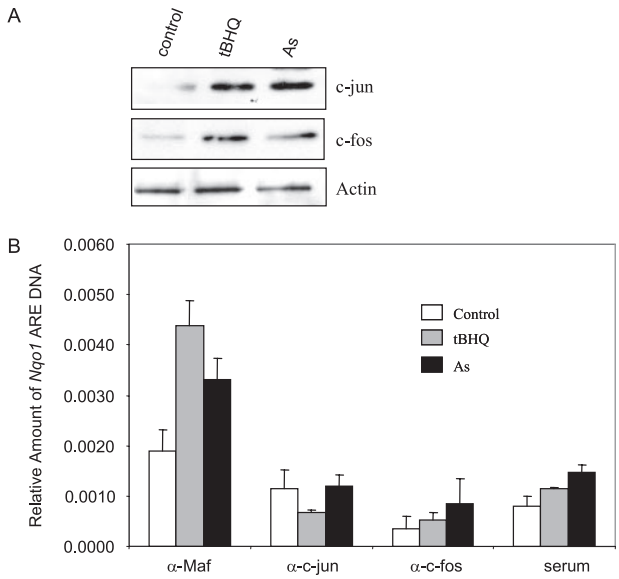

FIGURE 9. **Association of AP-1 proteins with *Nqo1* ARE.** *A*, protein expression of c-Jun, c-Fos, and actin in the presence of tBHQ (30 μM) or arsenic (*As*, 10 μM) for 4 h was examined by immunoblotting. *B*, association of c-Jun and c-Fos with *Nqo1* ARE in the absence or presence of tBHQ or arsenic was analyzed by ChIP assay with anti-c-Jun and anti-c-Fos, respectively. Anti-Maf and normal serum were included as positive and negative controls, respectively. Real-time PCR was performed to obtain quantitative results.

of AP-1 proteins c-Jun and c-Fos to the induction of *Nqo1* by arsenic were examined by ChIP. In Fig. 9*A*, the protein levels of c-Jun and c-Fos in the cells were first analyzed by immunoblotting. Both AP-1 proteins were detected constitutively. Arsenic or tBHQ increased the protein levels of the proteins. ChIP assays revealed that *Nqo1* ARE co-immunoprecipitated with c-Jun or c-Fos was similar in amount to that with serum control both in the absence or presence of the inducers (Fig. 9*B*). Association of ARE with Maf under the same condition was shown as a positive control. The data revealed that, whereas the protein levels of c-Jun and c-Fos were induced by arsenic or tBHQ, the AP-1 proteins were not associated with the *Nqo1* ARE in intact cells under basal conditions and were not recruited to the ARE enhancer of *Nqo1* upon induction by arsenic or tBHQ.

DISCUSSION

Mammalian cells cope with environmental toxic chemicals by adapting defense mechanisms that detoxify the toxicants, antagonize the toxic action, or both to maintain the chemical homeostasis and physiological function of the cells (28). One such mechanism is the Nrf2/Keap1/ARE target gene system that functions as a receptor/transcription factor/protein effector regulatory unit. The mechanics of the Nrf2/Keap1/ARE gene system consists of three steps; the cytoplasmic Nrf2/Keap1 senses the chemical changes in the cellular environment by interacting with the chemicals, Nrf2 transduces the signals by coordinated transcription of multiple ARE-controlled target genes in the nucleus, and finally, the induced xenobiotic-metabolizing enzymes and antioxidant proteins detoxify or antagonize the chemicals. Although the Nrf2 pathway has been implicated in defense against a number of oxidative and electrophilic chemicals, the role and mechanism of action of Nrf2 in cellular protection against toxic metals remain unclear.

The environmental soft metal arsenic causes a broad spectrum of toxicity in humans and animals (1, 3). To defend against arsenic, cells must develop complex adaptive responses. In this study we utilized genetic and biochemical approaches to demonstrate that arsenic potently induces *Nqo1* through the Nrf2-controlled, ARE-dependent transcription and, thus, identified the Nrf2/Keap1/ARE-driven genes regulatory unit as a key strategy of cellular defense against arsenic. Moreover, our findings revealed a unique signal transduction process involving sequential and dynamic protein-protein and protein-DNA interactions in the activation of Nrf2 by toxic metal.

Arsenic Stabilizes Nrf2 by Disrupting the Nuclear Nrf2·Keap1·Cul3 Complex—Quiescent Nrf2 resides in the cytoplasm and is rapidly degraded through the ubiquitin-26 S proteasome pathway. Ubiquitination of the cytoplasmic Nrf2, a key step of Nrf2 regulation, involves the Keap1·Cul3-dependent E3 (24–26). In a conceptual framework, Keap1 functions as a BTB-containing substrate adaptor protein for Cul3 that brings Nrf2 into the Cul3·Rbx1 complex for ubiquitination conjugation onto lysine residues located within the N-terminal Neh2 domain of Nrf2. However, the molecular events governing the activation of Nrf2 by various exogenous chemicals remain elusive. In particular, the role and interaction of Keap1·Cul3 with Nrf2 during Nrf2 activation have not been clearly addressed. One conventional view predicts that interaction of Keap1 with electrophilic or oxidant inducers

through its thiol groups triggers the dissociation of Nrf2 from the Nrf2·Keap1·Cul3 complex in the cytoplasm, thus keeping Nrf2 from ubiquitination by Keap1·Cul3. Alternatively, oxidative/electrophilic signals inhibit the ubiquitination activity of Keap1·Cul3 but not the association of Keap1 with Nrf2, thereby allowing newly synthesized Nrf2 to bypass Keap1·Cul3 and accumulate in the nucleus (39). Our data revealed that arsenic activates Nrf2 by inhibiting the protein turnover of Nrf2, extending the $t_{½}$ of Nrf2 from 21 to 200 min, which is consistent with the observations with oxidative/electrophilic inducers such as tBHQ. Others have reported up-regulation of the steady state level of Nrf2 protein by arsenic (36). In the cytoplasm, arsenic strongly inhibits the ubiquitination of Nrf2, but does not dissociate Nrf2 from Keap1 and Cul3. In contrast, Nrf2 was detected in association with Maf G/Maf K and the *Nqo1* ARE enhancer sequence but not with Keap1·Cul3 in the nucleus in the presence of arsenic. Pretreatment of cells with MG132 markedly increased the level of the Nrf2·Keap1·Cul3 association as detected by co-immunoprecipitation in both the cytoplasm and nucleus. However, the nuclear association was disrupted by arsenic. Thus, arsenic not only prevents the formation of new Nrf2·Keap1·Cul3 complex but also disrupts the existing complex in the nucleus. Our findings support a three step mechanism of Nrf2 activation by arsenic; (*a*) arsenic inhibits the ubiquitination of Nrf2 in the cytoplasm, possibly by inhibiting the ubiquitination activity of Keap1·Cul3 since arsenic does not disrupt the association of the cytoplasmic Nrf2 with Keap1·Cul3 but decreases the level of ubiquitinated Nrf2, (*b*) after nuclear translocation, Nrf2 dissociates from Keap1·Cul3 and forms heterodimer(s) with Maf G/Maf K, and (*c*) the Nrf2·Maf dimer is recruited to the ARE enhancer of *Nqo1*.

Our data revealed substantial differences between arsenic and tBHQ in Nrf2 activation. Notably, treatment with tBHQ did not affect the ubiquitination of Nrf2 in the cytoplasm as compared with arsenic. Furthermore, strong association of Nrf2 with Keap1·Cul3 was apparent in both the cytoplasm and nucleus of tBHQ-treated cells to a level comparable with that by MG132, whereas arsenic disrupted the association of Nrf2 with Keap1 and Cul3 in the nucleus. Nevertheless, tBHQ induced dimerization of Nrf2 with Maf G/Maf K (albeit at a much lower level than that of arsenic) and binding of Nrf2·Maf to *Nqo1* ARE enhancer. A simple explanation of the observation is that, whereas arsenic substantially disrupts the association of nuclear Nrf2 with Keap1·Cul3, tBHQ induces additional change(s) in the nucleus that permits dissociation of Nrf2 from a small fraction of the Nrf2·Keap1·Cul3 complex pool followed by dimerization of the freed Nrf2 with Maf and binding of Nrf2 to ARE. This notion is supported by the finding that tBHQ induced dimerization of Nrf2 and Maf at a level much lower than those induced by arsenic, MG132, or both (Fig. 8*B*). It has been noted that tBHQ induces phosphorylation of Nrf2 in addition to protein stabilization (40); whether such modification of Nrf2 accounts for the differential effects of arsenic and tBHQ on Nrf2 activation remains to be studied. Taken together, our findings revealed for the first time inducer-specific signaling events in the activation of Nrf2 by metal and antioxidant inducers.

Ubiquitination/Deubiquitination and Recycling of Keap1 during Nrf2 Activation—Keap1 appears to serve as a core component in the regulation of Nrf2, providing at least three functions; as a scaffold to anchor Nrf2 with the cytoskeleton filaments in the cytoplasm, as a Cul3 substrate adaptor to bring Nrf2 into the Cul3-dependent E3 complex for ubiquitination of Nrf2, and as a sensor to interact with oxidative/electrophilic stimuli for induction of target genes. Currently, information on the regulation of Keap1 itself is lacking. Low levels of ubiquitinated endogenous Keap1 were detected in the cytoplasm of cells treated with vehicle, arsenic, or tBHQ; treatment with MG132 substantially induced the ubiquitination of cytoplasmic Keap1 similarly to the ubiquitination of Nrf2. Ubiquitination of Keap1 in the nucleus was markedly reduced, suggesting a mechanism of deubiquitination of the protein. Thus, the pattern of Keap1 ubiquitination after the treatments was similar to that of Nrf2, with the exception that arsenic did not reduce the MG132-induced ubiquitination of keap1 as it did for Nrf2, suggesting overlapping mechanisms in the ubiquitination of the two proteins. Interestingly, Keap1 was constitutively expressed, and the protein level of Keap1 was not affected by treatments with arsenic, tBHQ, CHX, MG132, or combinations of the reagents, indicating that Keap1 is a stable protein and is not induced or down-regulated by arsenic or tBHQ in the cells tested. The findings are consistent with a model in which Keap1 serves as a substrate adaptor accepting polyubiquitin chains during the ubiquitination of Nrf2 by the Cul3-dependent E3 complex. In this scenario, ubiquitination of Keap1 does not target Keap1 for degradation by proteasomes. Rather, it is recycled for regulation of Nrf2; (*a*) in the absence of an inducer, Keap1 assists the ubiquitination and degradation of Nrf2, (*b*) in the presence of an inducer, Keap1 participates in the nuclear translocation of Nrf2, and (*c*) dissociation of Nrf2 from Keap1 and deubiquitination of Keap1 in the nucleus permits nuclear-cytoplasmic shuttling of Keap1. This model of Keap1 action is supported by a recent observation that blocking of nuclear protein export leads to nuclear accumulation of Keap1 (41).

Recruiting Nrf2·Maf Dimer to Nqo1 ARE Accounts for Both Basal and Inducible Expression of Nqo1—Mouse *Nqo1* is constitutively expressed and induced by oxidative and electrophilic chemicals in hepatocytes and intestinal epithelial cells. Both expressions require Nrf2 and ARE (19). The components of the protein complex binding ARE and mediating the transcription of endogenous *Nqo1* have been controversial. Nrf2 heterodimerizes with a small Maf protein (Maf G/Maf K), and the dimer binds to ARE *in vitro* (37). The role of the complex in the induction of endogenous *Nqo1* is not clear because cotransfection of Maf K with Nrf2 suppresses rather than enhances the transcription of the gene (37). In addition, Maf homodimers were postulated to suppress the *Nqo1* transcription through ARE in the absence of an inducer, whereas AP-1 proteins were suggested to compete with Nrf2 for binding ARE in the basal and inducible transcription of the gene due to apparent similarities between the ARE and the AP-1 DNA sequences (38). In either scenario "removal of negative factors" such as Maf homodimer or AP-1 proteins by Nrf2 serves as a main theme of induction of transcription. We tested the notion by examining the association of Nrf2 with Maf and with the endogenous *Nqo1*

ARE in intact cells by co-immunoprecipitation and ChIP assays. Our findings revealed that both Nrf2 and Maf G/Maf K were associated with the endogenous *Nqo1* ARE at comparable levels in the absence of arsenic or tBHQ, consistent with the notion that Nrf2 is required for the basal expression of *Nqo1*. The finding negates a role of Maf homodimer in the suppression of the basal expression. Both arsenic and tBHQ induced the dimerization of nuclear Nrf2, and Maf G/Maf K and markedly increased the binding of Nrf2·Maf to ARE. On the contrary, AP-1 proteins c-Fos and c-Jun, and Nrf2-binding proteins Keap1, Cul3, and ubiquitin were not co-immunoprecipitated with *Nqo1* ARE. Taken together, our data suggest an on-switch model of *Nqo1* transcription in which low occupancy of ARE by Nrf2·Maf controls the basal transcription, whereas inducers induce the stabilization and nuclear translocation of Nrf2 followed by the dimerization of Nrf2 with Maf G/Maf K and recruitment of the new Nrf2·Maf complex to ARE for induction. Given the fact that induction of *Nqo1* is prototypical of ARE-driven drug-metabolizing enzyme gene regulation in many aspects by a broad range of inducers, this model provides a framework for understanding the Nrf2/Keap1-mediated, ARE-dependent transcriptional regulation of protective enzyme/proteins by arsenic, other toxic metals, and oxidant/antioxidant chemicals.

Acknowledgments—We thank Drs. J. Antonini and F. Chen for National Institute for Occupational Safety and Health internal review of the manuscript.

REFERENCES

1. Gomez-Caminero, A., Howe, P., Hughes, M. F., Kenyon, E., Lewis, D. R., Moore, M., Ng, J., Aitio, A., and Becking, G. (2001) in *Environmental Health Criteria 224* (Ng, J., ed) 2nd Ed., World Health Organization, Geneva
2. Duker, A. A., Carranza, E. J., and Hale, M. (2005) *Environ. Int.* **31,** 631–641
3. Abernathy, C. O., Liu, Y. P., Longfellow, D., Aposhian, H. V., Beck, B., Fowler, B., Goyer, R., Menzer, R., Rossman, T., Thompson, C., and Waalkes, M. (1999) *Environ. Health Perspect.* **107,** 593–597
4. Tseng, C. H. (2005) *J. Environ. Sci. Health C Environ. Carcinog. Ecotoxicol. Rev.* **23,** 55–74
5. Chappell, W. R., Beck, B. D., Brown, K. G., Chaney, R., Cothern, R., Cothern, C. R., Irgolic, K. J., North, D. W., Thornton, I., and Tsongas, T. A. (1997) *Environ. Health Perspect.* **105,** 1060–1067
6. Taylor, P. R., Qiao, Y. L., Schatzkin, A., Yao, S. X., Lubin, J., Mao, B. L., Rao, J. Y., McAdams, M., Xuan, X. Z., and Li, J. Y. (1989) *Br. J. Ind. Med.* **46,** 881–886
7. Leonard, A., and Lauwerys, R. R. (1980) *Mutat. Res.* **75,** 49–62
8. Tabocova, S., Hunter, E. S., III, and Gladen, B. C. (1996) *Toxicol. Appl. Pharmacol.* **138,** 298–307
9. Golub, M. S., Macintosh, M. S., and Baumrind, N. (1998) *J. Toxicol. Environ. Health B. Crit. Rev.* **1,** 199–241
10. Mastin, J. P. (2005) *Cardiovasc. Toxicol.* **5,** 91–94
11. Evens, A. M., Tallman, M. S., and Gartenhaus, R. B. (2004) *Leuk. Res.* **28,** 891–900
12. Farber, E. M. (1992) *J. Am. Acad. Dermatol.* **27,** 640–645
13. Borst, P., and Ouellette, M. (1995) *Annu. Rev. Microbiol.* **49,** 427–460
14. Carter, N. S., and Fairlamb, A. H. (1993) *Nature* **361,** 173–176
15. Shi, W., Dong, J., Scott, R. A., Ksenzenko, M. Y., and Rosen, B. P. (1996) *J. Biol. Chem.* **271,** 9291–9297
16. Wood, T. C., Salavagionne, O. E., Mukherjee, B., Wang, L., Klumpp, A. F., Thomae, B. A., Eckloff, B. W., Schaid, D. J., Wieben, E. D., and Weinshilboum, R. M. (2006) *J. Biol. Chem.* **281,** 7364–7373
17. Mass, M. J., Tennant, A., Roop, B. C., Cullen, W. R., Styblo, M., Thomas, D. J., and Kligerman, A. D. (2001) *Chem. Res. Toxicol.* **14,** 355–361
18. Ernster, L., Estabrook, R. W., Hochstein, P., and Orrenius, S. (1987) *Chem. Scr.* **27,** 1–207
19. Ma, Q., Kinneer, K., Bi, Y., Chan, J. Y., and Kan, Y. W. (2004) *Biochem. J.* **377,** 205–213
20. Nguyen, T., Sherratt, P. J., and Pickett, C. B. (2003) *Annu. Rev. Pharmacol. Toxicol.* **43,** 233–260
21. Chan, K., Han, X. D., and Kan, Y. W. (2001) *Proc. Natl. Acad. Sci. U. S. A.* **98,** 4611–4616
22. Itoh, K., Chiba, T., Takahashi, S., Ishii, T., Igarashi, K., Katoh, Y., Oyake, T., Hayashi, N., Satoh, K., Hatayama, I., Yamamoto, M., and Nabeshima, Y. (1997) *Biochem. Biophys. Res. Commun.* **236,** 313–322
23. Nguyen, T., Yang, C. S., and Pickett, C. B. (2004) *Free Radic. Biol. Med.* **37,** 433–441
24. Kobayashi, A., Kang, M. I., Okawa, H., Ohtsuji, M., Zenke, Y., Chiba, T., Igarashi, K., and Yamamoto, M. (2004) *Mol. Cell. Biol.* **24,** 7130–7139
25. Cullinan, S. B., Gordan, J. D., Jin, J., Harper, J. W., and Diehl, J. A. (2004) *Mol. Cell. Biol.* **24,** 8477–8486
26. Zhang, D. D., Lo, S. C., Cross, J. V., Templeton, D. J., and Hannink, M. (2004) *Mol. Cell. Biol.* **24,** 10941–10953
27. Dinkova-Kostova, A. T., Holtzclaw, W. D., Cole, R. N., Itoh, K., Wakabayashi, N., Katoh, Y., Yamamoto, M., and Talalay, P. (2002) *Proc. Natl. Acad. Sci. U. S. A.* **99,** 11908–11913
28. Hu, X., Roberts, J. R., Apopa, P. L., Kan, Y. W., and Ma, Q. (2006) *Mol. Cell. Biol.* **26,** 940–954
29. Ramos-Gomez, M., Kwak, M. K., Dolan, P. M., Itoh, K., Yamamoto, M., Talalay, P., and Kensler, T. W. (2001) *Proc. Natl. Acad. Sci. U. S. A.* **98,** 3410–3415
30. Ma, Q., Battelli, L., and Hubbs, A. F. (2006) *Am. J. Pathol.* **168,** 1960–1974
31. Gao, X., and Talalay, P. (2004) *Proc. Natl. Acad. Sci. U. S. A.* **101,** 10446–10451
32. Ma, Q., and Baldwin, K. T. (2000) *J. Biol. Chem.* **275,** 8432–8438
33. Bianco, N. R., Chaplin, L. J., and Montano, M. M. (2005) *Biochem. J.* **385,** 279–287
34. Prochaska, H. J., and Santamaria, A. B. (1988) *Anal. Biochem.* **169,** 328–336
35. Zhang, D. D., Lo, S. C., Sun, Z., Habib, G. M., Lieberman, M. W., and Hannink, M. (2005) *J. Biol. Chem.* **280,** 30091–30099
36. Pi, J., Qu, W., Reece, J. M., Kumagai, Y., and Waalkes, M. P. (2003) *Exp. Cell Res.* **290,** 234–245
37. Nguyen, T., Huang, H. C., and Pickett, C. B. (2000) *J. Biol. Chem.* **275,** 15466–15473
38. Jaiswal, A. K. (1994) *Pharmacogenetics* **4,** 1–10
39. Kobayashi, A., Kang, M. I., Watai, Y., Tong, K. I., Shibata, T., Uchida, K., and Yamamoto, M. (2006) *Mol. Cell. Biol.* **26,** 221–229
40. Huang, H. C., Nguyen, T., and Pickett, C. B. (2002) *J. Biol. Chem.* **277,** 42769–42774
41. Nguyen, T., Sherratt, P. J., Nioi, P., Yang, C. S., and Pickett, C. B. (2005) *J. Biol. Chem.* **280,** 32485–32492